Back-propagation analysis for hypocenter location

Lejia Han, John C. Bancroft, and Joe Wong

ABSTRACT

The 2D and 3D approaches of back-propagation analysis are compared and evaluated in their applicability, computing intensity, noise tolerance, and efficiency for hypocenter location with synthetic data.

The 2D approach is limited to a vertical well monitoring scenario, while the 3D approach puts no limitation on the geometry of geophone arrays or observation wells. Both approaches are equivalent in terms of computing intensity, and both can achieve low location uncertainty.

INTRODUCTION

Software based on back-propagation analysis has been developed for hypocenter location using two approaches, one for 2D processing on data from a vertical well, and one for 3D processing on data from an arbitrary well or multiple wells. Both methods were implemented in MATLAB environment (Han, 2010).

The back-propagation analysis methodology and the implementation software has been investigated and tested with synthetic data for various geometries and parameters of our research interest such as the noise level and geophone spacing.

In this report, we will provide an overview of the integrated procedure and applied technologies, and emphasize some characteristics and differences between the two approaches in terms of applicability, computing intensity, noise tolerance, and efficiency for locating microseismic hypocenters.

METHODS, THEIR IMPLEMENTATION AND TESTING

The technologies applied in back-propagation analysis includes the modified energy ratio (MER) analysis for arrival time picking, weighted least squares for approximating the hodogram orientation, the nearest approach to two spatial lines for back-propagation analysis, and Student's t distribution approximation for determining the clustering of mutual intersections or nearest points. We also pre-process the raw data to attenuate random (Gaussian) noise with bandpass filtering, matched filtering, noise-signal separation, trace shifting, and stacking.

The integrated procedure and software of the above technologies was implemented within MATLAB for the 2D approach and the 3D approach. The 2D approach is processed in a radial section in the Cylindrical system, while the 3D approach is spatially implemented and coded in the the Cartesian system.

A synthetic data-generating procedure was also implemented to test the parameter sensitivity.

We will summarize below some characteristics and conclusions pertaining to our methodology. More details can be found in another CREWES resort (Han and Bancroft, 2010).

THE LIMITED APPLICABILITY WITH THE 2D APPROACH

The 2D approach is appropriate only for microseismic monitoring applications with a single vertical well; it is not appropriate for multiple vertical wells or any bent well, whether vertical, slanted, or horizontal.

The 2D approach uses a cylindrical coordinate system to project the 3C seismograms on both a radial plane and the map plane. With a homogenous and isotropic velocity model, propagation raypaths to a vertical array of geophones consist of a strict vertical plane if noise-free, as shown on the right of Figure 1(a), whereas raypaths on the map view coalesce into a single straight line, as shown on the right of Figure 1(b).
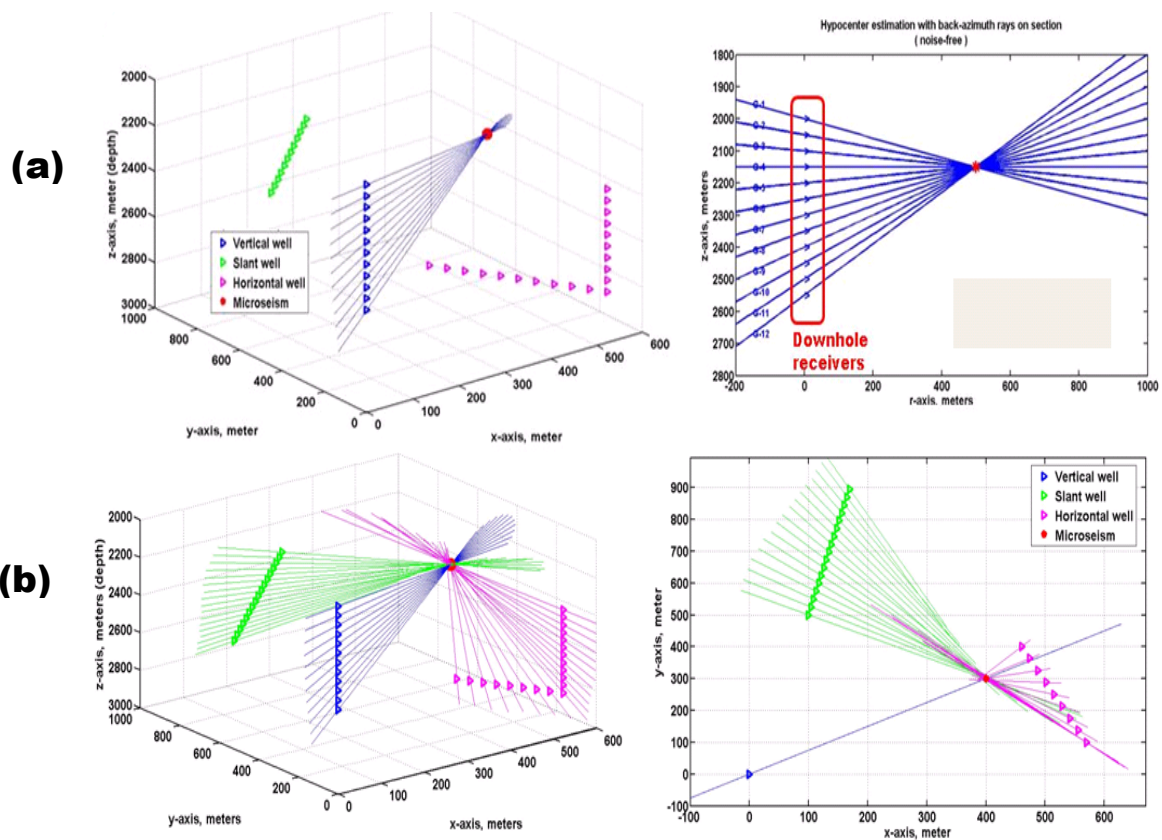

FIG.1 The applicability of 2D approach is limited in (a) to the single vertical well monitoring of 3C geophone, while the 3D approach in (b) can be applied to multi-well monitoring.

In contrast, the 3D approach puts no limit on the geometries of monitoring well, namely, it is applicable to arbitrary well, as shown in figure (b) either vertical (blue), or slant (green), or horizontal (pink). The difference is that raypaths from any non-vertical well either slant or horizontal will form a non-vertical plane at noise-free situation.

Figure 1(b) shows the propagation raypaths from three different observation wells monitoring a single microseism in a homogeneous and isotropic earth, resulting from a noise-free recording simulation.

THE EQUIVALENT COMPUTING INTENSITY OF 2D AND 3D APPROACHES

The computing intensity is equally low for either the 2D or 3D approach, as the underlying methods are essentially the same.

On 3C seismograms from a single vertical well, after first P-arrival picking with MER analysis and a set of noise attenuation processes, the back-propagation analysis is then accomplished on 2D planes with the cylindrical system by the 2D approach, while the 3D approach is implemented spatially in the Cartesian system. Both approaches require the following computations (here we are only concerned with computational efficiency; the matrices as defined in (Han, 2010) are not redefined here, but one induceded to illustrate the similarity in both methods, i.e.

1. The hodogram orientation by weighted least squares was implemented in the 2D approach with the following formulae:

$$k_m = (G_x{}^T W_m^T W_m G_x)^{-1} G_x{}^T W_m^T W_m d_y$$

$$k_r = (G_r{}^T W_r^T W_r G_r)^{-1} G_r{}^T W_r^T W_r d_z$$

where k_m and k_r represent the derived propagations in slopes on the map plane and the radial plane respectively; W_m and W_r, as well as G_x and G_r, are all matrices consisting of trace components, dy and dz are column vectors consisting of trace components.

Similarly, in the 3D approach, the hodogram orientation by weighted least squares again was implemented with the following formulae:

$$n_x = (G^T W_x^T W_x G)^{-1} G^T W_x^T W_x d_x$$

$$n_y = \left(G^T W_y^T W_y G\right)^{-1} G^T W_y^T W_y d_y$$

$$n_z = (G^T W_z^T W_z G)^{-1} G^T W_z^T W_z d_z$$

where n_x, n_y, and n_z represent propagation directions in unit cosines along the x, y, and z axis respectively; Wx, Wy, Wz, and G are all matrix consisting of trace components, dx, dy, and dz are column vectors consisting of trace components as well.

Hence, in general, the 2D and 3D approach has the equivalent computing intensity for hodogram orientation of the propagation directions respectively.

2. Another important computational step within both approaches determines for the intersections or the nearest points of all pairs of available propagation directions, generally by the following formula:

$$m_{svd} = V_p S_p^{-1} U_p^T d_g$$

where m_{svd} provides the information to deduce the intersections or the nearest point for the 2D and 3D approach respectively; *V*, *S*, and *U* are the singular value decomposition (SVD) components of the original matrix consisting of trace components, dg is a column vector consisting of geophone locations.

Therefore, both approaches are equivalent generally in computing the mutual intersections or the nearest points to non-intersecting lines.

3. The third computing step analyses the cluster of points which resulted from the above 2D and 3D calculations. As we only impose random noise in the testing data, we subject our data to Student's *t* distribution. The sample mean are used first to estimate the standard deviations, and then replaced by the modes of probability density functions in the following ways.

In the 2D approach, we use

$$f(l|n) = \frac{\Gamma\left(\frac{n+1}{2}\right)}{\Gamma\left(\frac{n}{2}\right)} \frac{1}{\sqrt{n\pi}} \frac{1}{\left(1 + \frac{l^2}{n}\right)^{\frac{n+1}{2}}}$$

$$f(r|n) = \frac{\Gamma\left(\frac{n+1}{2}\right)}{\Gamma\left(\frac{n}{2}\right)} \frac{1}{\sqrt{n\pi}} \frac{1}{\left(1 + \frac{r^2}{n}\right)^{\frac{n+1}{2}}}$$

$$f(z|n) = \frac{\Gamma\left(\frac{n+1}{2}\right)}{\Gamma\left(\frac{n}{2}\right)} \frac{1}{\sqrt{n\pi}} \frac{1}{\left(1 + \frac{z^2}{n}\right)^{\frac{n+1}{2}}}$$

where *f* represents the density function of *r*, *l* represents the raypaths on the map plane, *r* and *z* represent the raypath components along the radial and depth direction respectively; Γ represents the gamma function (i.e. $\Gamma(x) = \int_0^\infty \xi^{x-1} e^{-\xi} d\xi$), and *n* represents the sample number.

In the 3D approach, we use

$$f(x|n) = \frac{\Gamma\left(\frac{n+1}{2}\right)}{\Gamma\left(\frac{n}{2}\right)} \frac{1}{\sqrt{n\pi}} \frac{1}{\left(1 + \frac{x^2}{n}\right)^{\frac{n+1}{2}}}$$

$$f(y|n) = \frac{\Gamma\left(\frac{n+1}{2}\right)}{\Gamma\left(\frac{n}{2}\right)} \frac{1}{\sqrt{n\pi}} \frac{1}{\left(1 + \frac{y^2}{n}\right)^{\frac{n+1}{2}}}$$

$$f(z|n) = \frac{\Gamma\left(\frac{n+1}{2}\right)}{\Gamma\left(\frac{n}{2}\right)} \frac{1}{\sqrt{n\pi}} \frac{1}{\left(1+\frac{z^2}{n}\right)^{\frac{n+1}{2}}}$$

where *x*, *y*, and *z* represent the ***x-y-z*** components of the raypaths respectively; Γ represents the gamma function (i.e. $\Gamma(x) = \int_0^\infty \xi^{x-1} e^{-\xi} d\xi$), and n represents the sample number.

Two iterations of the above calculation were conducted on our experimental data to determine the clustering points that are surrounding the hypocenter.

The computation intensity is quite low in the sense that no regressing or recursive calculation is involved, whereas iteration is common in inversion and migration methodologies.

Although the calculations above are presented differently for the 2D and 3D approaches, they are essentially the same mathematical series.

Therefore, we can conclude that both approaches have an equivalently low computing intensity.

While the computing intensity in our applications is higher with the 3D approach due to the higher number of geophones and hence the statistical samples, the computing complexity is not. The 2D approach was tested with a single vertical well, whereas the 3D approach was tested with a 3-well monitoring scenario of a single microseism, as shown in Figure 2, although it would work with any pair of the three well types, or even a single well.
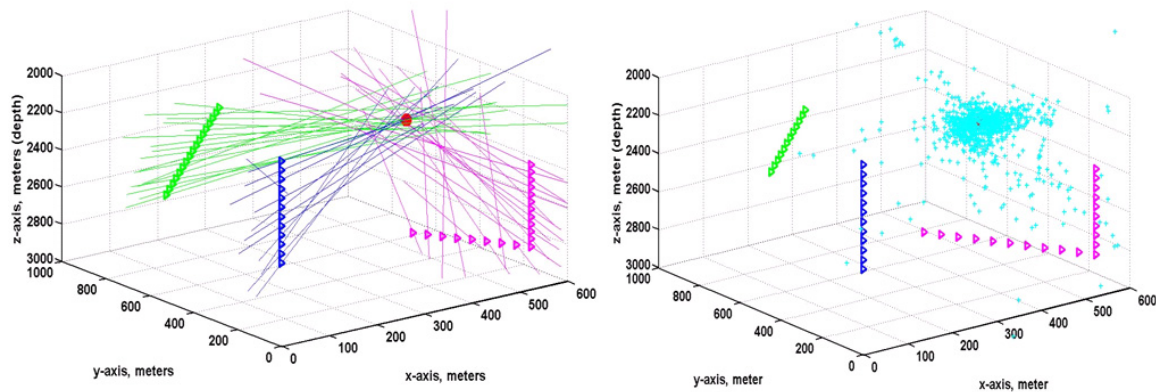

FIG.2 The back-propagation analysis with the 3D approach. There are 44 propagation raypaths from the 3 wells: vertical (blue), slant (green), and horizontal (pink). Hence, 946 intersections or nearest points are obtained from mutual pairs of all raypaths.

THE HIGHER NOISE TOLERANCE WITH THE 3D APPROACH

Improved noise tolerance is achieved by the picking accuracy of MER analysis, and the efficiency of noise attenuation processes being used in both 2D and 3D approaches.

MER analysis has demonstrated a higher picking accuracy than the standard STA/LTA method, as shown in Figure 3.
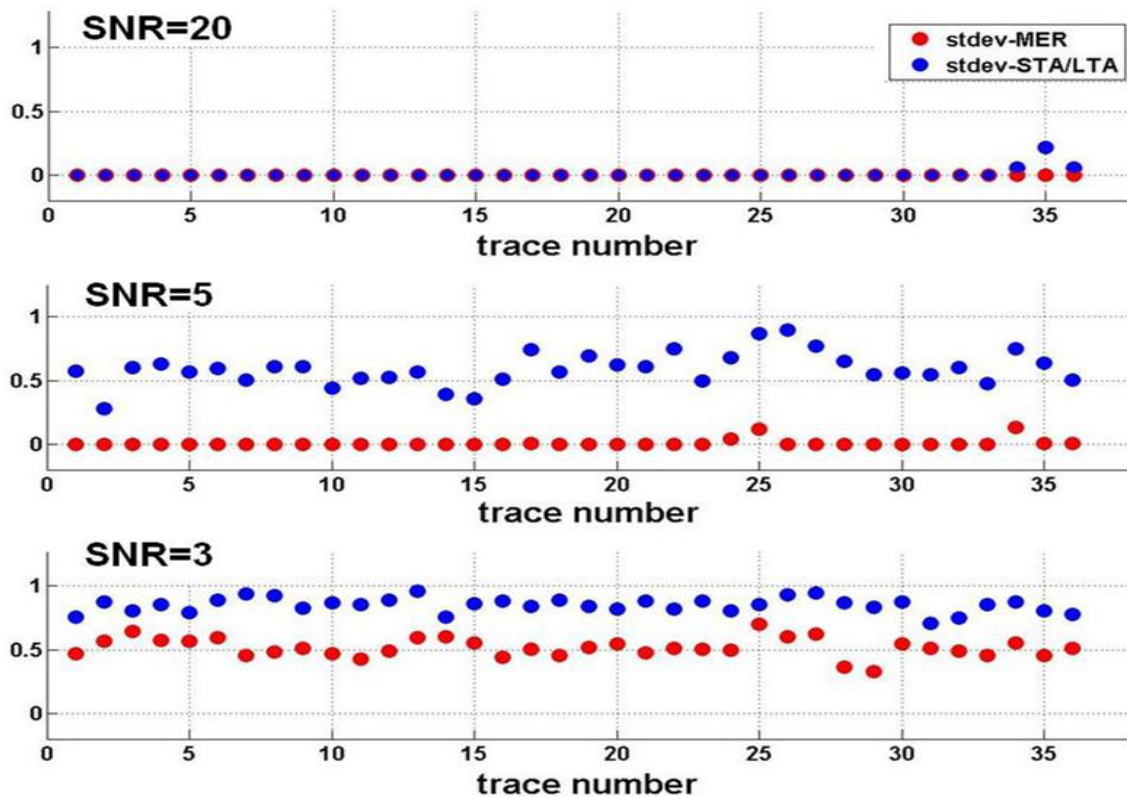

FIG.3 Comparisons of noise tolerance between MER analysis and the STA/LAT method at three noise levels, SNR=20, 5, and 3.

Further noise tolerance is obtained by the noise attenuation pre-process, as shown in figure 4. The processing pool includes the bandpass filtering (*f*-filter), matched filtering (*m*-filter), trace stacking, and noise-signal separation (NSS). On low noise data, the choice of f-filter, *m*-filter, and stacking might be enough.
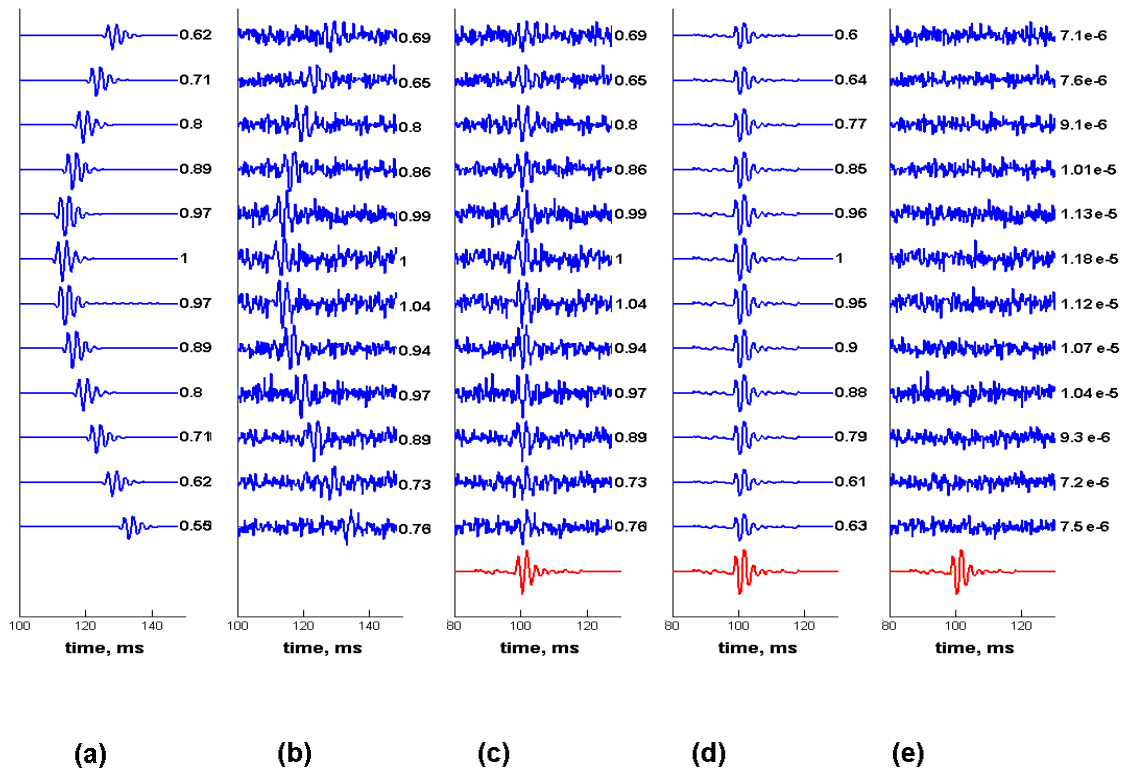
FIG.4 Noise attenuation and efficiency test. (a) seismograms of true waveforms; (b) noisy seismograms (c) noisy seismogram alignment after f-filter, m-filter, and MER shifting; the bottom red trace is the normalized stacking trace; (d) signal component of noisy traces after NSS; (e) separated Gaussian noise components after NSS.

However, the 3D approach has demonstrated a higher noise tolerance than the 2D approach during our extensive testing, as illustrated by Table 1 and Table 2. We believe that it is achieved by the statistical and spatial strengths the 3D approach has over the 2D approach, which may be further explained within the following context.

THE LOW LOCATION UNCERTAINTY WITH BOTH THE 2D AND 3D APPROACHES

The statistics of the location uncertainty are based on the synthetic data for 6 different situations in terms of noise level and geophone spacing. The 2D approach was investigated more extensively with 100 cases for each situation, resulting in 600 cases for all 6 situations, while the 3D approach was tested with only 30 cases for each situation, resulting in 180 cases for all 6 statistics.

Our research goal is to achieve a low location uncertainty at a noise level of SNR=3.

The 2D approach meets this demand with geophone spacings of 50 meters or 25 meters, but not at 10 meters, as shown in Table 1. However, the 3D approach exhibits the low uncertainty sustainably at all geophone displacements at the noise level of SNR=3, as shown in Table 2.

Although both approaches achieve ways for hypocenter location with low uncertainty, the 3D approach exhibits the more accurate location-estimations and the much lower standard deviations at all situations, in comparing Table 1 to Table 2. As both approaches have the essentially same methodology for first P-arrivals, noise tolerance, and back-propagation analysis, the reason of better performance with the 3D approach is attributed to statistical and spatial advantages.

The 2D approach is limited to single vertical well monitoring; therefore we cannot obtain enough statistical samples for an accurate and stable result. However, three wells are applied with the 3D approach; besides the statistical advantage, raypaths from three directions, produce an overlap volume containing the hypocenter. With wells chosen to form an approximately right angle with the expected hypocenter, improved results are expected.

However, the more wells that are used, the more expensive the experiment becomes, and at some level, there may be no a improvement in the quality of the final result. In that case, the 2D approach may become a practical and economic alternative.

Table 1: Statistics of location uncertainty results from 600 cases for 6 groups of parameters.

Statistics of the Location Uncertainty by the 2D Approach of Back-propagation Analysis

Noise	Spacing	Estimated	Hypocenter	Locations
SNR	dR (m)	Xs (m)	Ys (m)	Zs (m)
10	10	390 ± 28	292 ± 22	2148 ± 7
10	25	398 ± 13	298± 10	2151 ± 3
10	50	401 ± 8	301 ± 7	2149 ± 4
3	10	264 ± 58	195 ± 43	2122 ± 14
3	25	386 ± 37	286 ± 30	2151 ± 12
3	50	410 ± 27	301 ± 23	2152 ± 15
The True	Location:	400m	300m	2150m

Table 2: Statistics of location uncertainty results from 180 cases for 6 groups of parameters.

**Statistics of the Location Uncertainty
by the 3D Approach of Back-propagation Analysis**

Noise	Spacing	Estimated	Hypocenter	Locations
SNR	dR (m)	Xs (m)	Ys (m)	Zs (m)
10	10	400 ± 1.8	299 ± 2.2	2150± 2.1
10	25	400 ± 1.9	299± 1.7	2150 ± 1.7
10	50	400 ± 2.5	300 ± 2.4	2150 ±2.3
3	10	405 ± 9.0	294 ± 6.4	2153± 8.2
3	25	405 ± 5.0	295 ± 6.6	2155 ± 5.7
3	50	405 ± 7.7	299 ± 8.9	2158 ± 7.8
The True	Location:	400m	300m	2150m

FUTURE WORK

It would be interesting to have MER analysis with variable lengths of the energy-collecting window to accommodate more complicated cases than just picking on microseismograms usually containing only a single event on each trace.

Accuracy could be improved if back-propagation analysis were extended to a layered velocity model.

ACKNOWLEDGEMENTS

REFERENCES

Bancroft, J. C., Wong, J., and Han, L. (2010). Sensitivity measurements for locating microseismic events. CSEG Recorder, 35 , 27-36.

Han, L. (2010). Microseismic monitoring and hypocenter location. M.Sc. thesis, University of Calgary .

Han, L. and Bancroft, J. C. (2010). The nearest approach to multiple lines in n-dimensional space. CREWES Report, 21 , pp. 6.1-6.10.